

AN APPROXIMATE ANALYTIC TECHNIQUE FOR DETERMINING
THE OPERATING CHARACTERISTICS OF THERMIONIC
CONVERTERS IN THE IGNITED MODE*

James Keck
Massachusetts Institute of Technology
Consultant to
Thermo Electron Corporation

Abstract

An approximate analytic technique for solving the transport equations describing the diffusion region of a thermionic energy converter operating in the ignited mode has been developed. The method involves assuming a parametric form for the electron production and integrating the transport equations to determine the electron concentration, potential, and temperature distribution. These distributions are then used to determine the electron production from the ionization equation. Finally the parameters are adjusted to make the assumed production match the calculated production as closely as possible. In our initial investigations we have used a three parameter function of the form

$$d J_e / dx = A \tanh \left(\frac{x+a}{b} \right) \operatorname{sech}^2 \left(\frac{x+a}{b} \right).$$

The theory predicts qualitatively all the observed features of converter operation. In particular it predicts an optimum value for pd at which the arc drop in the plasma is a minimum. Limited quantitative comparisons also show reasonable agreement with experiments. The method may be systematically improved by assuming more complicated functional forms for the production term.

I. Introduction

The problem of determining the arc drop in the plasma of a thermionic energy converter operating in the ignited mode has been treated by many authors.⁽¹⁾ The basic equations governing the transport phenomena in the diffusion region of the plasma have been derived by Wilkins and Gyftopoulos⁽²⁾ and appropriate boundary conditions which apply across the sheaths have been set forth by Wilkins and McCandless.⁽³⁾

The solution of these equations has proved to be exceedingly difficult, however. The analytic techniques⁽⁴⁾ which have been presented previously employ numerous simplifying approximations which in general limit them to pressure-spacing products pd considerably greater than those of practical interest for power converters. On the other hand, the numerical "shooting" techniques⁽⁵⁾ which have been developed are subject to severe instabilities which make them exceedingly difficult and expensive to carry out. Moreover, numerical solutions give very little insight into the relative importance of the various physical phenomena and parameters which determine converter performance. Finally, none of

the existing treatments, either analytic or numerical, has predicted the experimentally observed optimum value of the pd product at which the arc drop across the plasma for fixed current is a minimum.

In this paper we present an approximate analytic method for solving the converter plasma equations which is very much simpler than the numerical "shooting" techniques and considerably more accurate than previous analytic treatments. It is based on assuming a parametric form for the net electron production in the converter. The transport equations may then be integrated to obtain the electron concentration, temperature, and potential energy distributions. These may in turn be used to calculate the corresponding net electron production from the ionization equation. Finally, the parameters in the assumed form are adjusted to make the assumed and calculated production agree as closely as possible. The success of the technique is determined by accuracy of the fit obtained. Systematic improvement of the results can be made by introducing progressively more complicated functional forms for the assumed production.

The basic equations and boundary conditions used in our analysis are presented in section II. The method of solution and the mathematical results are given in section III. The key element in the solution is a transcendental equation. A graphical method of solving this equation and some illustrative results are given in section IV. Finally section V briefly summarizes our conclusions.

II. Mathematical Model

A. Transport Equations

We shall consider a one dimensional three component plasma consisting of ion (i), electron (e), and neutrals (n). We assume low degrees of ionization so that

$$n_e = n_i \ll n_n, \quad (2.1)$$

where n_α is the concentration of species α , and equality of ion and neutral temperatures so that

$$\Theta_i = \Theta_n \quad (2.2)$$

where $\Theta_\alpha = kT_\alpha$. For such a plasma, the equation of state is

$$p = n_e (\Theta_e + \Theta_n) + n_n \Theta_n \approx n_n \Theta_n \quad (2.3)$$

* This work was supported by the U. S. Atomic Energy Commission under Contract AT(30-1)-4125.

and the transport equations are⁽²⁾

$$\frac{d\Gamma_e}{dx} = \frac{d\Gamma_i}{dx} = S, \quad (2.4)$$

$$\frac{\Gamma_e}{\mu_e} = -\frac{dp_e}{dx} - n_e \frac{d\psi}{dx}, \quad (2.5)$$

$$\frac{\Gamma_i}{\mu_i} = -\frac{dp_i}{dx} + n_e \frac{d\psi}{dx}, \quad (2.6)$$

$$Q_e = \Gamma_e \left(\frac{5}{2} \Theta_e + \psi \right) - 2 n_e \mu_e \Theta_e \frac{d\Theta_e}{dx}, \quad (2.7)$$

$$Q_n = -2 n_n \mu_n \Theta_n \frac{d\Theta_n}{dx}, \quad (2.8)$$

where Γ_α , Q_α , p_α and μ_α are the particle flux, energy flux, pressure and mobility of species α , S is the net ionization rate, and ψ is the potential energy of an electron. The mobilities are related to the collision cross-sections $\sigma_{\alpha\beta}$ for species α and β by

$$\mu_{en}^{-1} = m_e \bar{c}_e (\sigma_{en} n_n + \sigma_{ei} n_e) \quad (2.9)$$

$$\mu_{in}^{-1} = \sqrt{2} m_n \bar{c}_n \sigma_{in} n_n, \quad (2.10)$$

$$\mu_{nn}^{-1} = \sqrt{2} m_n \bar{c}_n \sigma_{nn} n_n, \quad (2.11)$$

where m_α is the mass and

$$\bar{c}_\alpha = (8 \Theta_\alpha / \pi m_\alpha)^{1/2} \quad (2.12)$$

is the mean thermal speed of species α . Note that in the above equations we have omitted the thermal diffusion terms and the forces arising from the transfer of directed momentum from electrons to ions. We have also assumed that the energy flux carried by ions is negligible compared to that carried by neutrals.

If we further assume that radiation losses and energy transfer from electrons to heavy particles are small, then we have for neutrals

$$dQ_n/dx = 0 \quad (2.13)$$

and for electrons

$$dQ_e/dx = -V_i S, \quad (2.14)$$

where V_i is the ionization potential.

For collisional ionization and threebody recombination the net ionization rate is

$$S = \beta_r n_e (n_s^2 - n_e^2) \quad (2.15)$$

where

$$\beta_r \text{ (cm}^6/\text{m)} \approx 4 \times 10^{-27} [\Theta_e \text{ (eV)}]^{-9/2} \quad (2.16)$$

is the threebody recombination rate constant⁽⁶⁾ and

$$n_s = n_n^{1/2} \left(\frac{m_e \Theta_e}{2\pi \hbar^2} \right)^{3/4} e^{-V_i/2\Theta_e} \quad (2.17)$$

is the Saha electron concentration. Over a reasonable range about a reference temperature Θ_e^* , n_s can be well approximated by

$$n_s \approx n_e^* e^{-V^*/\Theta_e}, \quad (2.18)$$

where

$$n_e^* = n_n^{1/2} \left(\frac{2.72 m_e \Theta_e^*}{2\pi \hbar^2} \right)^{3/4} \quad (2.19)$$

and

$$V^* = \frac{1}{2} V_i + \frac{3}{4} \Theta_e^* \quad (2.20)$$

B. Boundary Conditions

We assume a motive diagram of the type shown in Figure 1. Under these conditions the emitter boundary conditions are⁽³⁾

$$\Gamma_{eo} = \Gamma_E - (R_{eo} - \frac{1}{2}\Gamma_{eo}) e^{-V_E/\Theta_{eo}}, \quad (2.21)$$

$$\Gamma_{io} = -2R_{io}, \quad (2.22)$$

$$Q_{eo} = \Gamma_E (2\Theta_E + V_E) - (\Gamma_E - \Gamma_{eo}) (2\Theta_{eo} + V_E), \quad (2.23)$$

and the collector boundary conditions are

$$\Gamma_{ed} = (R_{ed} + \frac{1}{2}\Gamma_{ed}) e^{-V_C/\Theta_{ed}}, \quad (2.24)$$

$$\Gamma_{id} = 2R_{id}, \quad (2.25)$$

$$Q_{ed} = \Gamma_{ed} (2\Theta_{ed} + V_C + \psi_d), \quad (2.26)$$

where Γ_E is the emitter saturation current and

$$R_\alpha = n_\alpha \bar{c}_\alpha / 4 \quad (2.27)$$

is the random current for species α . Note that we have assumed back emission from the collector is negligible.

The arc drop obtained from inspection of Figure 1 is

$$V_D = V_o - V = V_E - V_C - \psi_d \quad (2.28)$$

where

$$V_o = \phi_E - \phi_C \quad (2.29)$$

is the contact potential.

III. Method of Solution

A. Temperature Distribution for Neutrals

We shall begin by considering the temperatures of the neutrals since this determines both the ion temperature and the neutral particle density which will be needed later. Substituting (2.3), (2.11), and (2.12) into (2.8) and integrating we find for constant σ_{nn}

$$\Theta_n = \Theta_E [1 - \eta (1 - \epsilon_{CE}^{3/2})]^{2/3}, \quad (3.1)$$

where

$$n = x/d \quad (3.2)$$

is a dimensionless distance and

$$\epsilon_{CE} = \Theta_C / \Theta_E \quad (3.3)$$

is the ratio of collector and emitter temperatures.

The corresponding heat flux carried by the neutrals is

$$Q_n = \frac{\pi}{6\sqrt{2}} \left(\frac{\Theta_E}{\sigma_{nn} d} \right) \left(\frac{8\Theta_E}{\pi m_n} \right)^{1/2} (1 - \epsilon_{CE}^{3/2}). \quad (3.4)$$

B. Electron Density Distribution

To obtain an approximate analytic solution for the electron concentration, we assume that the net electron production S given by (2.15) can be approximated by a function of the form

$$S^* = A \tanh \left(\frac{\eta + a}{b} \right) \operatorname{sech}^2 \left(\frac{\eta + a}{b} \right) \quad (3.5)$$

where A , a , and b are parameters which will be adjusted later to give the best fit of S and S^* . Obviously, this choice of S^* is by no means unique and more complicated functional forms could be used which might give better results. The reasons for choosing this particular form for our initial investigation are 1) it has a shape which is physically reasonable, 2) it approximates quite well the forms obtained in previous numerical investigations, and 3) it is relatively simple and convenient to integrate. It should be emphasized, however, that the success of this or any other form for S^* can only be determined a posteriori by assessing the accuracy of the fit to S .

Substituting S^* for S in (2.4) and integrating we obtain

$$\begin{aligned} \Gamma_i &= \Gamma_e - \Gamma \\ &= \Gamma_{id} + \frac{1}{2} Abd \left[\tanh^2 \left(\frac{\eta + a}{b} \right) - \tanh^2 \left(\frac{1+a}{b} \right) \right] \end{aligned} \quad (3.6)$$

where $\Gamma = J/e$ is the converter current divided by the electronic charge. Adding (2.5) and (2.6) and using (2.9), (2.10), (2.12), (2.25), (2.27) and (3.2) gives

$$\frac{d\bar{P}}{dn} + d_{ei} \bar{P} = -d_{in} (\bar{\Gamma}_i + \epsilon_{ei}), \quad (3.7)$$

where

$$\bar{P} = n (\Theta_e + \Theta_i) / n_{ed} (\Theta_{ed} + \Theta_C), \quad (3.8)$$

$$\bar{\Gamma}_i = \Gamma_i / \Gamma_{id}, \quad (3.9)$$

$$d_{ei} = \frac{8\Gamma_{ed} \sigma_{ei} d \Theta_e}{\pi \bar{c}_e (\Theta_e + \Theta_i)}, \quad (3.10)$$

$$d_{in} = \frac{4\sigma_{in} pd}{\pi (\Theta_{ed} + \Theta_C)} \left(\frac{2\Theta_C}{\Theta_i} \right)^{1/2}, \quad (3.11)$$

$$\epsilon_{ei} = \frac{\Gamma_{ed} \sigma_{en}}{R_{ed} \sigma_{in}} \left(\frac{\Theta_{ed} \Theta_e}{8\Theta_C \Theta_i} \right)^{1/2}, \quad (3.12)$$

and we used the approximation $\Gamma_e \approx \Gamma_{ed}$. Note d_{ei} and d_{in} are essentially the converter spacing divided by the electron-ion and ion-neutral mean free paths respectively while ϵ_{ei} is the ratio of the ion-neutral to electron-neutral mean free paths.

Before attempting to integrate (3.7) it is useful to estimate the magnitude of the coefficients d_{ei} , d_{in} and ϵ_{ei} . Using the cross-sections⁽⁷⁾ summarized in Table 1 and the reference conditions $T_{e0} \sim T_{ed} \sim 1.5 T_E \sim 4.0 T_C \sim 2800^\circ K$ and $\Gamma \sim R_{ed}$ we find

$$d_{ei} \approx Jd \text{ (mil a/cm}^2\text{)}/700, \quad (3.13)$$

$$d_{in} \approx 1.1 \text{ pd (mil torr)}, \quad (3.14)$$

$$\text{and } \epsilon_{ei} \approx 1/3, \quad (3.15)$$

where we have assumed $\Theta_i \approx \sqrt{\Theta_E \Theta_C}$.

It can be seen from (3.13) that for $Jd \ll 700$ mil a/cm², which is the range of interest for most practical converters, the term proportional to d_{ei} in (3.7) will be small. It can also be seen from (3.15) that the dependence on ϵ_{ei} is relatively weak. Thus, since the temperature dependence of σ_{in} is relatively weak, it is a good first approximation to drop the term proportional to d_{ei} and assume d_{in} and ϵ_{ei} are constant. (3.7) can then easily be integrated to give

$$\begin{aligned} \bar{P} &= 1 + \bar{d} \left\{ [1 + B \operatorname{sech}^2 \left(\frac{1+a}{b} \right)] \left(\frac{1-\eta}{1+a} \right) \right. \\ &\quad \left. - B \left(\frac{b}{1+a} \right) \left[\tanh \left(\frac{1+a}{b} \right) - \tanh \left(\frac{\eta+a}{b} \right) \right] \right\}, \end{aligned} \quad (3.16)$$

where

$$\bar{d} = (1+a) (1 + \epsilon_{ei}) d_{in} \quad (3.17)$$

and

$$B = Abd/2 \Gamma_{id} (1 + \epsilon_{ei}). \quad (3.18)$$

We can now obtain an expression for the electron production in terms of \bar{P} by substituting (3.8) into (2.15). This gives

$$S = (2J_{id}/d) d_r \bar{P} (\bar{P}_S^2 - \bar{P}^2) \quad (3.19)$$

where

$$\bar{P}_S = n_S (\Theta_e + \Theta_i) / n_{ed} (\Theta_{ed} + \Theta_C) \quad (3.20)$$

and

$$d_r = \frac{\beta_r n_{ed}^2 d}{\bar{c}_{id}} \left(\frac{\Theta_{ed} + \Theta_C}{\Theta_e + \Theta_i} \right)^3 \quad (3.21)$$

Note d_r is essentially the converter spacing divided by the mean free path for ion recombination at the collector.

To determine the parameters B , a , and b we require that S given by (3.19) fit S^* given by (3.5) as closely as possible. A simple (but not necessarily the best) method of doing this is to match S and S^* at the extrapolated end point $\eta = -a$ and at the point of maximum electron production $\eta = \eta_1$. Matching at

the extrapolated end point requires $S(-a) = S^*(-a) = 0$ which gives

$$1 + \bar{d} [1 + B \operatorname{sech}^2 \left(\frac{1+a}{b} \right) - B \left(\frac{b}{1+a} \right) \tanh \left(\frac{1+a}{b} \right)] = 0 \quad (3.22)$$

Matching the positions of the maximum electron production requires $(dS/d\eta) = (dS^*/d\eta) = 0$ which gives

$$[(\bar{P}_S^2 - 3\bar{P}^2) \frac{d\bar{P}}{d\eta} + 2\bar{P}\bar{P}_S \frac{d\bar{P}_S}{d\eta}]_1 = 0 \quad (3.23)$$

and

$$(\eta_1 + a)/b = \delta_1 = \coth^{-1} \sqrt{3} \quad (3.24)$$

where the subscript 1 denotes quantities evaluated at $\eta = \eta_1$. Note that in differentiating (3.19) we have neglected the temperature dependence of d_{r1} in comparison with that of \bar{P}_S . Finally, matching the values of S and S^* at the $\eta = \eta_1$ gives

$$2B(1 + \epsilon_{ei})/b \sqrt{3} = d_{r1} \bar{P}_1 (\bar{P}_{S1}^2 - \bar{P}_1^2) \quad (3.25)$$

where we have used (3.18) and (3.24).

The three equations (3.22), (3.23), and (3.25) are sufficient to determine the unknown parameters B , a , and b . An additional equation which can be used to determine \bar{P}_{S1} can be obtained by substituting the boundary conditions (2.22) and (2.25) into (3.6) and using (2.12), (2.27), (3.8), (3.9), and (3.18). This gives

$$\begin{aligned} \bar{\Gamma}_{i0} &= -\bar{P}_0 (\theta_{ed} + \theta_C) / (\theta_{eo} + \theta_E) \sqrt{\epsilon_{CE}} \\ &= 1 + B(1 + \epsilon_{ei}) \left[\tanh^2 \left(\frac{a}{b} \right) - \tanh^2 \left(\frac{1+a}{b} \right) \right] \end{aligned} \quad (3.26)$$

To solve this set of equations, it is convenient to introduce the variable

$$(\eta + a)/b = \delta \quad (3.27)$$

We then obtain from (3.16) and (3.22)

$$B = (\bar{d} + 1) \delta_d \coth \delta_d \sqrt{\bar{d}} (1 - C) \quad (3.28)$$

and

$$\bar{P} = (\bar{d}/\delta_d) (B \tanh \delta - D\delta), \quad (3.29)$$

where

$$\delta_d = (1 + a)/b, \quad (3.30)$$

$$C = 2 \delta_d / \sinh 2\delta_d \quad (3.31)$$

and

$$\begin{aligned} D &= 1 + B \operatorname{sech}^2 \delta_d \\ &= (\bar{d} + C) \sqrt{\bar{d}} (1 - C) \end{aligned} \quad (3.32)$$

Combining (3.29) with (3.17) and (3.25) and using (3.28) and (3.30) - (3.32) we obtain

$$\left(\frac{\bar{P}_S}{\bar{P}} \right)_1^2 = 1 + \frac{2E^2}{\epsilon_r \bar{d}^2 (\bar{d} + 1)^2} \quad (3.33)$$

where

$$E = \frac{(1 - C) \delta_d}{\coth \delta_d} \left[1 - 1.14 \frac{D}{B} \right]^{\frac{3}{2}} \quad (3.34)$$

and

$$\begin{aligned} \epsilon_r &= d_{r1}/d_{in} (1 + \epsilon_{ei})^2 \\ &= \frac{\pi \beta_{r1} n_{ed}^2 (\theta_{ed} + \theta_C) (\theta_{ed} \theta_i)^{\frac{1}{2}}}{4\sqrt{2} \sigma_{in} \bar{c}_{ed} p \theta_C (1 + \epsilon_{ei})^2} \left(\frac{m_n}{m_e} \right)^{\frac{1}{2}} \\ &= \left(\frac{\theta_{ed} + \theta_C}{\theta_{ei} + \theta_{i1}} \right)^3 \end{aligned} \quad (3.35)$$

Note ϵ_r is essentially the ratio of the ion neutral mean free path to the ion recombination length at the collector. For the reference conditions $T_{eo} \sim T_{ed} \sim 1.5 T_E \sim 4.0 T_C \sim 2800^\circ \text{K}$ and $\Gamma \sim (n_e \bar{c}_e/4)/d$

$$\epsilon_r \approx 3 \times 10^{-7} J^2 (a^2/\text{cm}^4)/p (\text{torr}) \quad (3.36)$$

so that for typical operating conditions ϵ_r is very small. Substituting (3.33) into (3.23) gives

$$\begin{aligned} \Delta \chi &= - (d \ln \bar{P}_S / d\eta)_1 \\ &= \left(\frac{E^2 - \epsilon_r \bar{d}^2 (\bar{d} + 1)^2}{E^2 + \frac{1}{2} \epsilon_r \bar{d}^2 (\bar{d} + 1)^2} \right) F \end{aligned} \quad (3.37)$$

where

$$\begin{aligned} F &= \frac{1}{2} (d \ln \bar{P} / d\eta), \\ &= \frac{\delta_d - 3(\bar{d} + C)/2(\bar{d} + 1)}{\sqrt{3}(1 + a)(1 - 1.14 D/B)} \end{aligned} \quad (3.38)$$

To obtain the extrapolated end point a , we first observe that for $\eta = 0$, (3.28) gives

$$\bar{P}_0 = (\bar{d}/\delta_d) (B \tanh \delta_0 - D \delta_0) \quad (3.39)$$

where from (3.27)

$$a = b \delta_0 = \delta_0 / (\delta_d + \delta_0). \quad (3.40)$$

We next anticipate that for most conditions of interest $\delta_0 \coth \delta_0 - 1 \ll \delta_d \coth \delta_d - 1$ so that

$$\bar{P}_0 \approx (\bar{d}/\delta_d) (B - D) \tanh \delta_0 \quad (3.41)$$

Substituting (3.41) into (3.26) and using (3.30) and (3.40) we obtain

$$B(1 + \epsilon_{ei}) \tanh^2 \delta_0 + G \tanh \delta_0 - H = 0 \quad (3.42)$$

which may be solved to give

$$\tanh \delta_0 = \frac{G}{2B(1 + \epsilon_{ei})} \left[\left(1 + \frac{4B(1 + \epsilon_{ei})H}{G^2} \right)^{\frac{1}{2}} - 1 \right] \quad (3.43)$$

where

$$G = \left(\frac{\theta_{ed} + \theta_C}{\theta_{eo} + \theta_E} \right) \frac{\bar{d}(B - D)}{\sqrt{\epsilon_{CE}} \delta_d} \quad (3.44)$$

and

$$H = B(1 + \epsilon_{ei}) \tanh^2 \delta_d - 1. \quad (3.45)$$

For $G^2 \gg 4B(1 + \epsilon_{ei})G$, which corresponds to

$$\delta_d \ll (\bar{d} + 1)/2 \sqrt{\epsilon_{CE}} (1 + \epsilon_{ei}),$$

$$\delta_o \approx H/G \quad (3.46)$$

and

$$\bar{P}_o \approx \sqrt{\epsilon_{CE}} (\theta_{eo} + \theta_E/\theta_{ed} + \theta_C) H, \quad (3.47)$$

while for $G^2 \ll 4B(1 + \epsilon_{ei})H$, corresponding to δ_d
 $\gg (\bar{d} + 1)/2 \sqrt{\epsilon_{CE}} (1 + \epsilon_{ei})$,

$$\delta_o \approx \frac{1}{2} \ln(4H/G) \quad (3.48)$$

and

$$\bar{P}_o \approx \bar{d} + 1. \quad (3.49)$$

Using (3.28), (3.31) and (3.32) it can be seen from (3.46) and (3.48) that for $\bar{d} > 1$ the approximation $\delta_o \coth \delta_o - 1 \ll \delta_d \coth \delta_d - 1$ used to obtain (3.42) is valid for all δ_d .

This completes the determination of the parameters necessary to specify the electron concentration and we may now use our results to calculate the electron potential energy and electron temperature distributions.

C. Electron Potential Energy

To obtain an equation for the electron potential energy we use (2.5) and the equation $p_i = p_e \theta_i/\theta_e$ to eliminate dp_i/dx from (2.6). Then using (2.9), (2.10), (2.12), (2.25), (2.27), (3.2), (3.8), (3.9), (3.11), and (3.12) and the approximation $\mu_i \ll \mu_e$ we find

$$\frac{d\psi}{d\eta} = \frac{d_{in}}{P} (\bar{\Gamma}_i \theta_e - \epsilon_{ei} \theta_i) + \theta_e \frac{d}{d\eta} \ln \left(1 + \frac{\theta_i}{\theta_e}\right). \quad (3.50)$$

We then substitute (3.27), (3.30) and (3.45) into (3.6)' to obtain

$$\bar{\Gamma}_i = -H + B(1 + \epsilon_{ei}) \tanh^2 \delta \quad (3.51)$$

Using (3.51) and (3.29), (3.50) may now be formally integrated to give

$$\psi_d = \psi_1 + \psi_2 + \psi_3 \quad (3.52)$$

where

$$\psi_1 = \int_0^1 \theta_e \left[\frac{d}{d\eta} \ln \left(1 + \frac{\theta_i}{\theta_e}\right) \right] d\eta \approx \theta_C - \theta_E \quad (3.53)$$

$$\psi_2 = \int_{\delta_o}^{\delta_d} \frac{(\theta_e I - \epsilon_{ei} \theta_i) \tanh^2 \delta \, d\delta}{(1 + \epsilon_{ei}) (B \tanh \delta - D\delta)} \quad (3.54)$$

and

$$\psi_3 = - \int_{\delta_o}^{\delta_d} \frac{(\theta_e H + \epsilon_{ei} \theta_i) \operatorname{sech}^2 \delta \, d\delta}{(1 + \epsilon_{ei}) (B \tanh \delta - D\delta)}, \quad (3.55)$$

where

$$I = B(1 + \epsilon_{ei}) \operatorname{sech}^2 \delta_d + 1. \quad (3.56)$$

To evaluate ψ_2 we observe that the integrand is a rapidly increasing function of δ so that the major contribution to the integral comes from the vicinity of the end point δ_d . Thus, it is a good approximation to set $\tanh \delta \approx \tanh \delta_d$ and $\theta_e I - \epsilon_{ei} \theta_i \approx \theta_{ed} I - \epsilon_{ei} \theta_C$ and using (3.28) we obtain

$$\psi_2 \approx \left(\frac{\theta_{ed} I - \epsilon_{ei} \theta_C}{(1 + \epsilon_{ei}) D} \right) (\tanh^2 \delta_d) \ln \left(\frac{\bar{d} + 1}{1 - C} \right) \quad (3.57)$$

where we have assumed $\delta_o \ll \delta_d$.

To evaluate ψ_3 we proceed in a similar manner and observe first the important contribution to the integral in this case comes from the vicinity of the end point δ_o where it is a good approximation to set $\tanh \delta = \delta$ and $\theta_e H + \epsilon_{ei} \theta_i \approx \theta_{eo} H + \epsilon_{ei} \theta_E$. We thus obtain

$$\psi_3 \approx - \left(\frac{\theta_{eo} H + \epsilon_{ei} \theta_E}{(1 + \epsilon_{ei}) (B - D)} \right) \ln \left(\frac{\tanh \delta_d}{\tanh \delta_o} \right) \quad (3.58)$$

D. Electron Temperature

The electron temperature may now be determined from (2.7) which using (2.9), (2.10), (2.12), (2.25), (2.27), (3.2), (3.8), (3.10), (3.11), and (3.12) can be written

$$\frac{d\theta_e}{d\eta} = \frac{1}{2} \left(1 + \frac{\theta_i}{\theta_e}\right) \left(\frac{\epsilon_{ei} d_{in}}{P} + d_{ei} \right) \left(\frac{5}{2} \theta_e + \psi - \frac{Q_e}{\Gamma_e} \right). \quad (3.59)$$

In principle this equation can be integrated using the same techniques employed in the preceding section. Since this is somewhat complicated, however, we shall not attempt it in the present analysis and instead we shall assume that to a first approximation:

$$d\theta_e/d\eta = -\Delta\theta_e \quad (3.60)$$

where $\Delta\theta_e = \theta_{eo} - \theta_{ed}$ is a constant. Then using (3.60) and the boundary condition (2.26) we find

$$\ln \left(\frac{R_{ed}}{\Gamma_{ed}} + \frac{1}{2} \right) = \frac{1}{2} + \frac{2 \Delta \theta_e}{(\theta_{ed} + \theta_C) (\epsilon_{ei} d_{in} + d_{ei})} \quad (3.61)$$

From (3.12) we see that ϵ_{ei} contains the factor Γ_{ed}/R_{ed} so that (3.61) is an implicit rather than explicit equation for R_{ed}/Γ_{ed} . However, for $2\Delta\theta \ll (\theta_{ed} + \theta_C) (\epsilon_{ei} d_{in} + d_{ei})$, it is an excellent approximation to evaluate ϵ_{ei} at $R_{ed}/\Gamma_{ed} = \exp(1/2) - 1/2 = 1.15$.

At this point we note that since \bar{P}_S is a function of θ_e we have in effect three unknowns: θ_{eo} , $\Delta\theta_e$, and δ_d and two equations (3.32) and (3.35) which relate to them. To obtain a third equation which will permit us to solve the set we subtract (2.26) from (2.23) which gives

$$Q_{eo} - Q_{ed} = 2\Gamma_E (\theta_E - \theta_{eo}) + (\Gamma_{eo} - \Gamma_{ed}) (2\theta_{eo} + V_E) + \Gamma_{ed} (2\Delta\theta_e + V_E - V_C - \psi_d). \quad (3.62)$$

Integrating (2.4) and (2.14) we find

$$\Gamma_{ed} - \Gamma_{eo} = \Gamma_{id} - \Gamma_{io} \quad (3.63)$$

and

$$Q_{eo} - Q_{ed} = V_i (\Gamma_{id} - \Gamma_{io}). \quad (3.64)$$

Substituting (3.63) and (3.64) into (3.62) and using (2.28), (3.6), and (3.9), then gives

$$(V_i + 2\theta_{eo} + V_E) \epsilon_m (1 - \bar{\Gamma}_{io}) = 2(\Gamma_E/\Gamma_{ed}) (\theta_E - \theta_{eo}) + 2\Delta\theta_e + V_E - V_C - \psi_d, \quad (3.65)$$

where from (2.25), (2.27), and (2.12)

$$\epsilon_m = \frac{\Gamma_{id}}{\Gamma_{ed}} = 2 \left(\frac{R_{ed}}{\Gamma_{ed}} \right) \left(\frac{m_e \theta_C}{m_n \theta_{ed}} \right)^{\frac{1}{2}} \approx \frac{1}{500}. \quad (3.66)$$

From (2.21) and (2.24) we find

$$V_C = \theta_{ed} \ln \left(\frac{R_{ed}}{\Gamma_{ed}} + \frac{1}{2} \right) \quad (3.67)$$

and

$$V_E = \theta_{eo} \ln \left(\frac{R_{eo}}{\Gamma_{eo}} - \frac{1}{2} \right) \left(\frac{\Gamma_E}{\Gamma_{eo}} - 1 \right)^{-1}, \quad (3.68)$$

where from (2.12), (2.25), (2.27), (3.6), (3.9), (3.63) and (3.66) we have

$$\frac{R_{eo}}{\Gamma_{eo}} = -\bar{\Gamma}_{io} \sqrt{\epsilon_{CE}} \left(\frac{\theta_{eo}}{\theta_{ed}} \right)^{\frac{1}{2}} \left(\frac{R_{ed}}{\Gamma_{ed}} \right) \left(\frac{\Gamma_{ed}}{\Gamma_{eo}} \right) \quad (3.69)$$

and

$$\frac{\Gamma_{eo}}{\Gamma_{ed}} = 1 - \epsilon_m (1 - \bar{\Gamma}_{io}). \quad (3.70)$$

Finally, from (2.18), (2.19), (3.24), (3.28), (3.29), (3.33), (3.34), (3.37) and (3.60) we find

$$\theta_{eo} = \theta_{ed} + \Delta\theta_e = \theta_{e1} + \eta_1 \Delta\theta_e \quad (3.71)$$

$$\Delta\theta_C = \theta_{e1} \Delta\chi/\chi_1 \quad (3.72)$$

$$\theta_{e1} = V^*/\chi_1 \quad (3.73)$$

when

$$\chi_1 = N + \ln \left(\frac{\bar{d}}{\delta d} \right) (1 - 1.14 \frac{D}{B})^{\frac{1}{2}} \left(1 + \frac{\epsilon_r \bar{d}^2 (\bar{d}+1)^2}{2E^2} \right)^{-1} \quad (3.74)$$

and

$$N = \ln \left(\frac{3\epsilon_r}{2} \right)^{\frac{1}{2}} \frac{n^* (\theta_{e1} + \theta_{i1})}{n_{ed} (\theta_{ed} + \theta_C)}$$

$$= \frac{1}{2} \ln \left(\frac{2.72 m_e \theta^*}{\pi \hbar^2} \right)^{\frac{3}{2}} \left(\frac{m_n \theta_{ed}}{m_e \theta_i} \right)^{\frac{1}{2}} \times$$

$$\frac{3\pi \beta_{ri} (\theta_{ed} + \theta_C)^2}{32 \sigma_{in} \bar{\epsilon}_{ed} (1 + \epsilon_{ei}) \theta_C (\theta_{e1} + \theta_{i1})} \quad (3.75)$$

For our reference conditions, $\theta^* \sim \theta_{e1} \sim \theta_{ed} \sim 1.5 \theta_E \sim 4 \theta_C \sim 2800^\circ\text{K}$.

$$N \approx 7.8 \quad (3.76)$$

We now observe that by means of the equations developed in this section all quantities in (3.65) can be found as functions of Γ_E/Γ_{eo} and δ_d . Thus given Γ_E/Γ_{eo} we can solve (3.65) either graphically or numerically to obtain δ_d which in turn determines all other variables.

E. Current-Voltage Characteristics

Using (3.6), (3.66) and (3.70), the ratio of the total current to the emitter electron current is found to be

$$\Gamma/\Gamma_{eo} = (1 - \epsilon_m)/[1 - \epsilon_m (1 - \bar{\Gamma}_{io})] \quad (3.77)$$

The arc drop may be determined from (2.28) and (3.65) and is given by

$$\begin{aligned} V_D &= V_E - V_C - \psi_d \\ &= 2(\Gamma_E/\Gamma_{eo}) (\theta_{eo} - \theta_E) - 2\Delta\theta_e \\ &\quad + (V_i + 2\theta_{eo} + V_E) \epsilon_m (1 - \bar{\Gamma}_{io}). \end{aligned} \quad (3.78)$$

IV. Graphical Solution and Illustration Results

To obtain a graphical solution for the equations of the previous section, we substitute (3.67) - (3.73) into (3.65) and solve for $\Delta\chi$. This gives

$$\Delta\chi = \chi_1 [Q - (\chi_1/\chi_E)P]/(1 + R - \eta_1 Q) \quad (3.79)$$

where

$$Q = \frac{\Gamma_E}{\Gamma_{eo}} + \frac{1}{2} \ln \left(\frac{\Gamma_E}{\Gamma_{eo}} - 1 \right) \left(1 + \frac{\Gamma_{ed}}{2R_{ed}} \right) \left(1 - \frac{\Gamma_{eo}}{2R_{eo}} \right)^{-1} \left(1 - \frac{D}{B} \right)^{-1}$$

$$- \frac{1}{2} \left(\frac{\epsilon_{ei} - I \operatorname{sech}^2 \delta_d}{D(1 + \epsilon_{ei})} \right) \ln \left(\frac{\bar{d} + 1}{1 - C} \right) \quad (3.80)$$

$$- \frac{1}{2} \left(\frac{\epsilon_{ei}}{(B - D)(1 + \epsilon_{ei})} \right) \ln \left(\frac{\coth \delta_o}{\coth \delta_d} \right),$$

$$P = (\Gamma_E/\Gamma_{eo}) - \chi_E \epsilon_m (1 - \bar{\Gamma}_{io}) \quad (3.81)$$

$$- \epsilon_{CE} \left(\frac{\epsilon_{ei} \tanh^2 \delta_d}{D(1 + \epsilon_{ei})} \right) \ln \left(\frac{\bar{d} + 1}{1 - C} \right)$$

$$- \left(\frac{\epsilon_{ei}}{(B - D)(1 + \epsilon_{ei})} \right) \ln \left(\frac{\coth \delta_o}{\coth \delta_d} \right),$$

$$R = \frac{1}{2} \left(\frac{1}{1 + \epsilon_{ei}} \right) \ln \left(\frac{\bar{d} + 1}{1 - C} \right), \quad (3.82)$$

and

$$\chi_E = V^*/\Theta_E. \quad (3.83)$$

In deriving (3.79) - (3.82) we have used (3.26), (3.28) and (3.41) to eliminate Γ_{i0} in certain terms. We have also assumed $\Delta\Theta_e < \Theta_{e0} \ll V_i$ and dropped several terms which are small as a consequence.

Equation (3.79) may now be solved simultaneous with (3.37) by plotting them both as a function of δ_d . This is illustrated in Figure 2 for the case $J_E/J = 2$. The curves identified by the parameters $\sqrt{\epsilon_r d}$ ($\bar{d} + 1$) were obtained from (3.37) while those identified by $(\bar{d} + 1)$ were obtained from (3.79). For given ϵ_r and \bar{d} , the value of δ_d is determined by the intersection of the corresponding pair of curves. The root of interest is the largest one. The physical significance, if any, of the smaller roots is not clear at the present time. Once δ_d is determined, all other variables may be obtained from the equations of the preceding section.

Figure (3a) shows curves for the Saha electron concentration n_S , the actual electron concentration n_e , the ion current J_i as a function of position in the converter for typical operating conditions. All these quantities exhibit the characteristic shapes found in previous numerical solutions⁽⁵⁾ of the problem. The two expressions S and S^* for the net electron production are compared in Figure (3b) and it can be seen that the fit is very satisfactory.

Figure (4) shows the electron and ion temperatures as a function of position in the converter for the same conditions as Figure (3). Note that the electron temperature is a linear function of x/d because the gradient was assumed constant in the analysis. The ion temperature, however, was obtained by integration of the neutral heat flux equation and is not linear due to variations in the thermal conductivity with temperature. The electric field is essentially the product of the ion current density and the electrical resistivity. It rises rapidly in the vicinity of the collector because the low electron density in this region results in a high effective resistivity. A similar effect of opposite sign occurs at the emitter.

The emitter and collector electron temperatures are shown in Figure (4a) as a function of the pd product for $J_E/J = 2$. It can be seen that the emitter electron temperature has a minimum in the neighborhood of $pd = 20$ and rises for both smaller and larger pd . The physical reason for this is that for small pd electron loss by ambipolar diffusion to the walls is large and consequently the temperature must rise to maintain the ionization required to carry the prescribed current. On the other hand, for large pd a higher electron temperature is required at the emitter to provide the electron concentration gradient necessary to drive the current through a larger effective resistance. For the same reasons the collector temperatures exhibit a maximum.

The calculated arc drop V_D is compared with experimental results⁽⁸⁾ in Figure (4b) for the same conditions as those in Figure (4a). A value of 0.5 ev

was assumed for the contact potential in the experiments. Both the calculated and experimental curves clearly show the existence of an optimum pd at which the arc drop in the converter plasma is a minimum. The calculated value of this minimum based on the cross-sections given in Table I is 0.27 ev which agrees well with recent experimental estimates.⁽⁹⁾ The slopes of the calculated and experimental curves at large pd are also in good agreement. This confirms the value of the ion-neutral cross-section which is the most important parameter for determining the slope. This is a result of the fact that the diffusion is ambipolar. Thus, the electron and ions must move together and since the ion-neutral mean free path is smaller than either the electron-neutral or electron-ion mean free paths most of the resistance is due to the ions. As a consequence, accurate values of the ion-neutral mean free path are of considerable importance in determining converter performance.

Calculations of the current-voltage characteristics can be made in the same manner. However, due to a tendency for positive and negative terms to cancel for large and small values of Γ_E/Γ_{e0} they are somewhat more difficult to carry out graphically and are currently being programmed for a numerical computer. In this connection we may note that all the results presented in this paper were obtained by hand computation using a slide rule.

V. Concluding Remarks

On the basis of the analysis presented in this paper we conclude that the approximate analytic technique described can be a very useful tool for the investigation of thermionic energy converters operating in the ignited mode. The method is very much simpler and more efficient than numerical integration and more general and accurate than previous analytic treatments. It gives considerable qualitative insight into the importance and effect of the various physical parameters which determine converter performance and provides the first detailed explanation of an optimum pd product at which the arc drop in the plasma is a minimum. The quantitative comparisons which have been made show reasonable agreement with experiments and with further refinement the method should give results at least as reliable as the input data.

The most questionable approximation made in the present treatment is the assumption of a constant electron temperature gradient. Although this is reasonable for small gradients, it's effect is difficult to estimate for large gradients. The approximation can be removed by integrating the energy equation and while this would complicate the analysis somewhat, it should increase the reliability of the results considerably. This is an important improvement which should be made before serious quantitative applications of the method are made.

In addition, the present analysis is limited to the case of monotonic emitter and collector sheaths of the type illustrated in Figure 1, and the possibility of work function changes due to the Schottky

effect at large negative voltages has not been considered. Finally, we have neglected radiation losses and diffusion of excited species in the cascade ionization process. Although the effect of these latter approximations is thought to be small in the range of interest for practical converters, they also need further study.

References

1. For summary and references see R. H. Bullis, L. K. Hansen, C. Warner, J. M. Houston, M. F. Koskinen, and N. S. Rasor, *J. Appl. Phys.* 38, 3425 (1967).
2. D. R. Wilkins and E. P. Gyftopoulos, *J. Appl. Phys.* 7, 2888 (1966).
3. R. J. McCandless, D. R. Wilkins, and S. L. Derby, Theory of Thermionic Converter Volume Phenomena, IEEE Conference Record of 1969 Thermionic Conversion Specialist Conference, (Institute of Electrical and Electronics Engineers, New York, 1969). Alternatively, D. R. Wilkins and R. J. McCandless, "Thermionic Converter Plasma Analysis," GE SP-9004 (Nuclear Thermionic Power Operation, General Electric Company, Pleasanton, 1969).
4. N. S. Rasor, "Analytical Correlation of Cesium Diode Phenomenology," Report International Conference on Thermionic Electric Power Generation (London, 1965).
5. D. Lieb and W. Bornhorst, Plasma Analysis, Chap. 2 in Final Report Research in Thermionic Conversion, TE 4072-49-68 (Thermo Electron Corp., Waltham, 1967); C. Warner and L. K. Hansen, Fourth Annual Technical Summary Report for Basic Research in Thermionic Energy Conversion, Chaps. 3 and 4, AI-64-271 (Atomics International, North American Aviation, Canoga Park, 1964); Technical Summary Report for Basic Research in Thermionic Energy Conversion, Chaps. 3-6, AI-65-191 (Atomics International, North American Aviation, Canoga Park, 1965); R. J. McCandless, D. R. Wilkins, and S. L. Derby, loc. cit.
6. Peter Mansbach and James Keck, *Phys. Rev.*, 181, 275 (1969).
7. J. M. Houston, "Cross Section Values to Use in Analyzing the Cesium Thermionic Converter," 300, Report on the Thermionic Conversion Specialist Conference, (Institute of Electrical and Electronics Engineers, New York, 1964).
8. S. Kitrilakis, F. Rufe, D. Lieb, L. van Someren, J. Weinstein, Final Report for the Thermionic Research Program, 1, IX-24 (Thermo Electron, Waltham, 1965).
9. F. Rufe and D. Lieb, "The Dependence of the Volt-Ampere Characteristics on Collector Temperature," in IEEE Conference Record of 1969, Thermionic Conversion Specialist Conference, 237, (Institute of Electrical and Electronics Engineers, New York, 1969).

TABLE 1
SUMMARY OF CROSS SECTIONS⁽⁷⁾

$\sigma_{in} \approx 1200 \text{ A}^2$
$\sigma_{en} \approx 400 \text{ A}^2$
$\sigma_{nn} \approx 100 \text{ A}^2$
$\sigma_{ei} = \left(\frac{\pi^2}{16}\right) \left(\frac{e^2}{kT_e}\right)^2 \ln \Lambda_e \sim 10^4 \text{ A}^2$

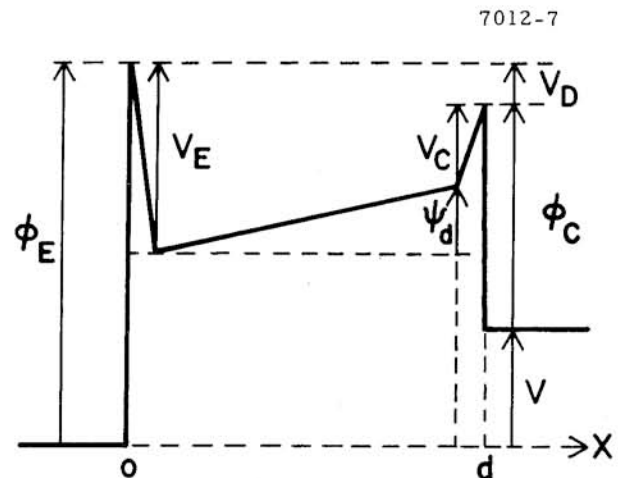


Figure 1. Schematic illustration of motive diagram assumed in the analysis.

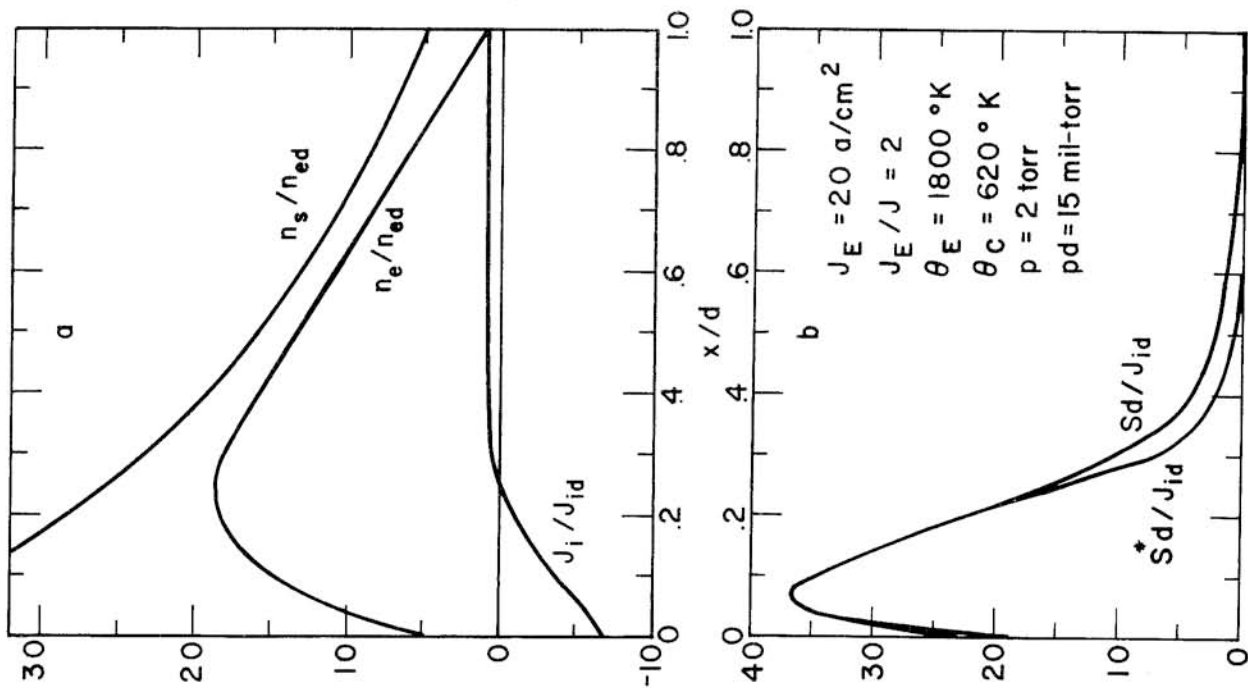


Figure 3. a. Calculated distributions for Saha electron concentration n_s , electron concentration n_e , and ion current J_i .
 b. Comparison of assumed and calculated expressions for the net electron production. The conditions for (a) and (b) are the same.

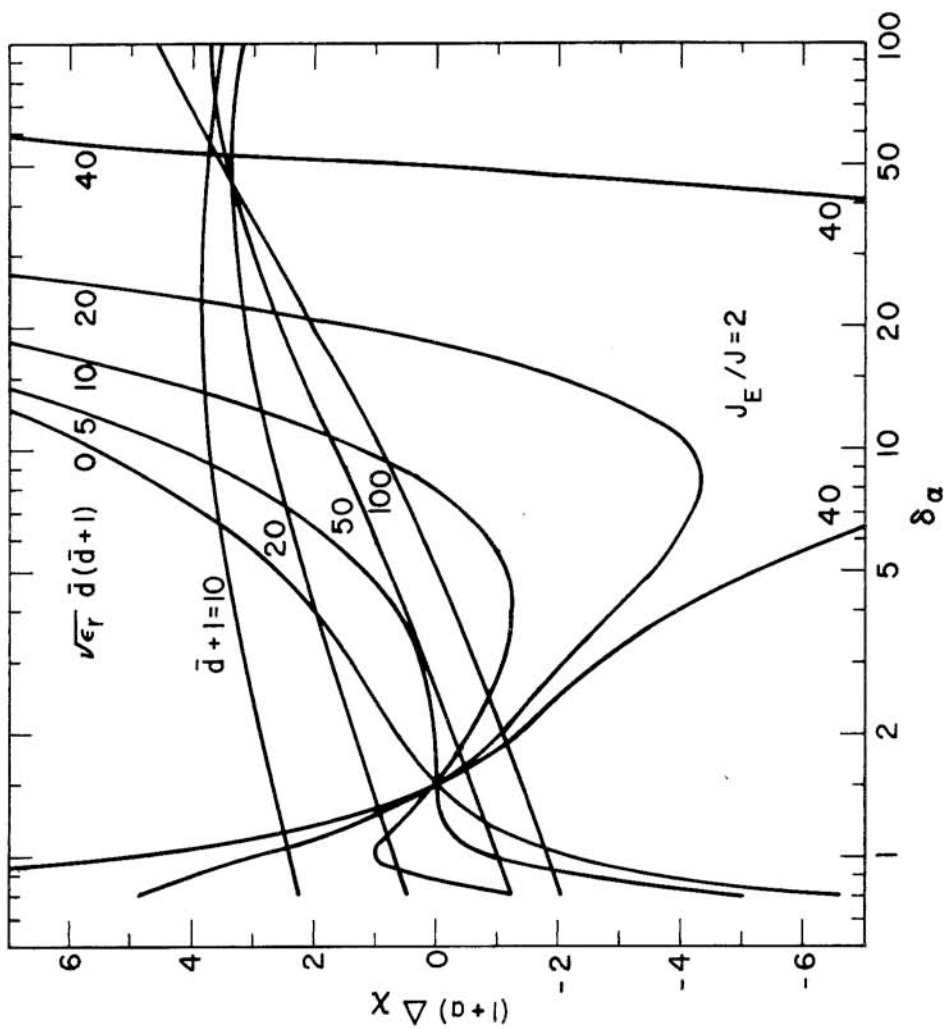


Figure 2. Illustration of graphical solution of equations (3.37) and (3.79) for $J_E/J = 2$. See text for discussion.

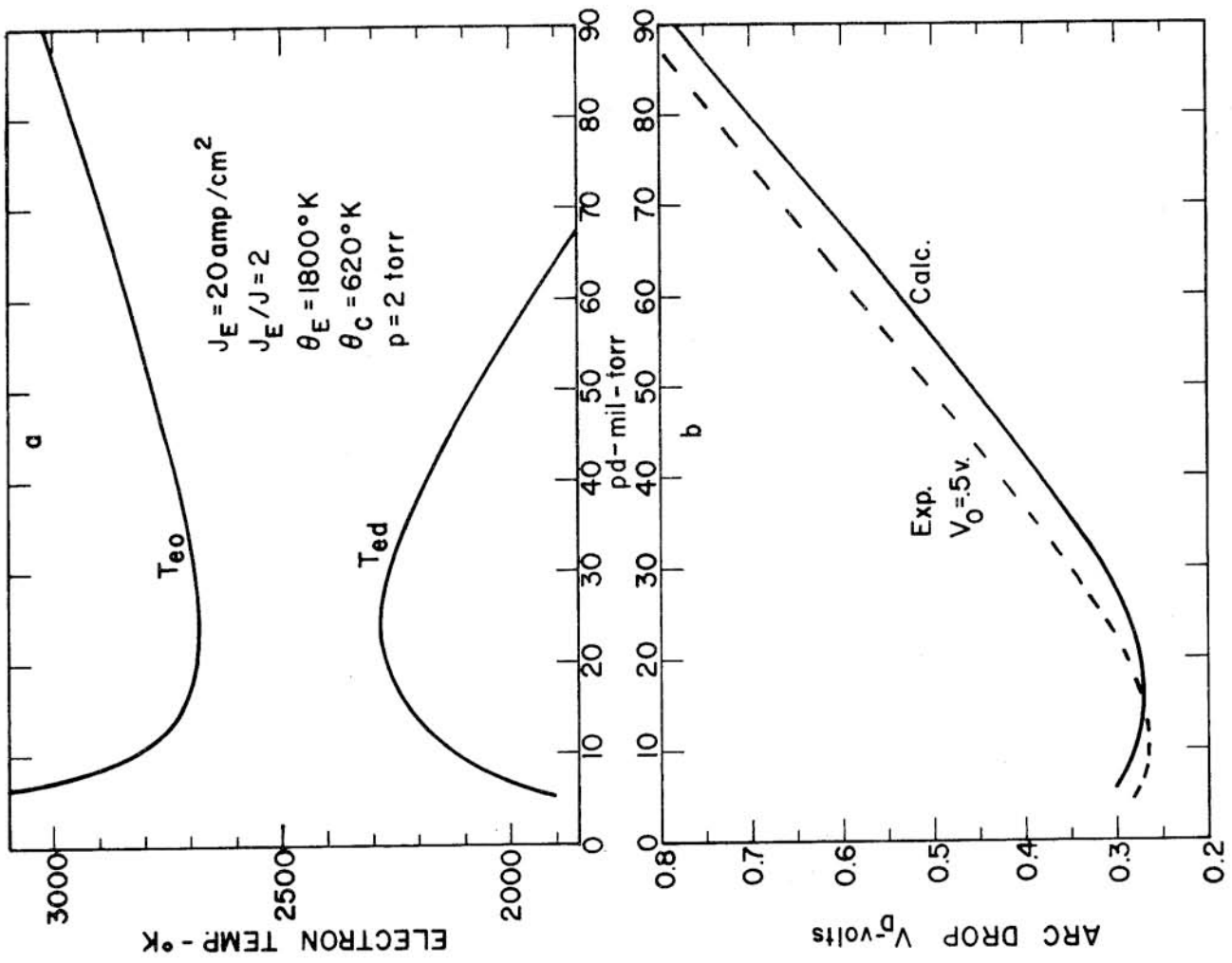


Figure 5. a. Emitter and collector temperatures as a function of pd for fixed current.

b. Comparison of calculated and measured arc drop as a function of pd for the same condition as (a). A contact potential $V_0 = 0.5 \text{ v}$ was assumed for calculating V_D from the experimental results. Note the existence of an optimum pd in the range 10-20 at which the output voltage is a maximum.

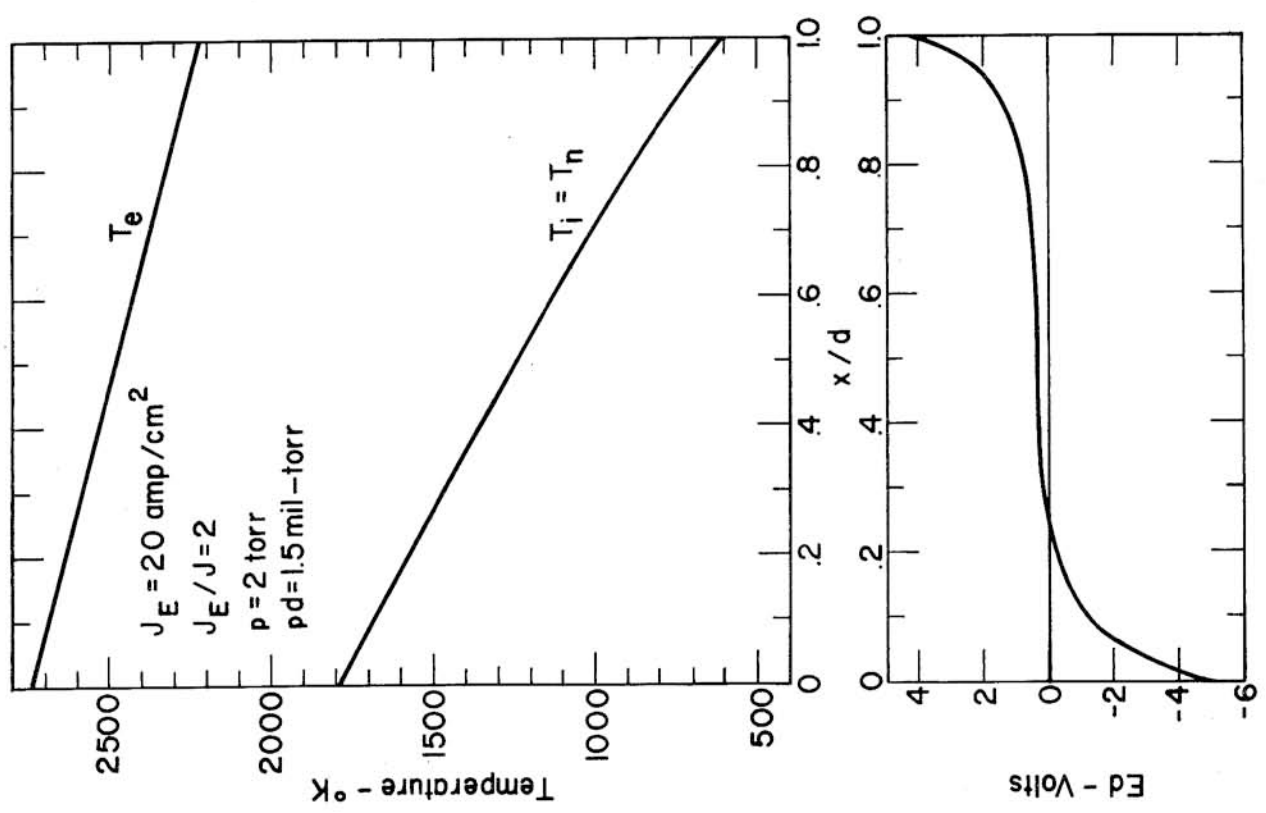


Figure 4. Calculated distributions for electron, ion, and neutral temperatures T_e , T_i , and T_n and electric field spacing product ed. Note T_i was assumed equal to T_n in the analysis.